Molecular Therapy
Nucleic Acids
Original Article

miR-196a enhances polymerization of neuronal microfilaments through suppressing IMP3 and upregulating IGF2 in Huntington's disease

Han-In Yang,[1,4] Pin-Yu Huang,[1,4] Siew Chin Chan,[1,2,4] Chih-Wei Tung,[1,2,4] Pei-Hsun Cheng,[1] Chuan-Mu Chen,[3] and Shang-Hsun Yang[1,2]

[1]Department of Physiology, College of Medicine, National Cheng Kung University, Tainan 70101, Taiwan; [2]Institute of Basic Medical Sciences, College of Medicine, National Cheng Kung University, Tainan 70101, Taiwan; [3]Department of Life Sciences, College of Life Sciences, National Chung Hsing University, Taichung 40227, Taiwan

Huntington's disease (HD) is one of the inheritable neurodegenerative diseases, and these diseases share several similar pathological characteristics, such as abnormal neuronal morphology. miR-196a is a potential target to provide neuroprotective functions, and has been reported to enhance polymerization of neuronal microtubules in HD. While microtubules and microfilaments are two important components of the neuronal cytoskeleton, whether miR-196a improves neuronal microfilaments is still unknown. Here, we identify insulin-like growth factor 2 mRNA binding protein 3 (IMP3), and show that miR-196a directly suppresses IMP3 to increase neurite outgrowth in neurons. In addition, IMP3 disturbs neurite outgrowth *in vitro* and *in vivo*, and worsens the microfilament polymerization. Moreover, insulin-like growth factor-II (IGF2) is identified as the downstream target of IMP3, and miR-196a downregulates IMP3 to upregulate IGF2, which increases microfilamental filopodia numbers and activates Cdc42 to increase neurite outgrowth. Besides, miR-196a increases neurite outgrowth through IGF2 in different HD models. Finally, higher expression of IMP3 and lower expression IGF2 are observed in HD transgenic mice and patients, and increase the formation of aggregates in the HD cell model. Taken together, miR-196a enhances polymerization of neuronal microfilaments through suppressing IMP3 and upregulating IGF2 in HD, supporting the neuroprotective functions of miR-196a through neuronal cytoskeleton in HD.

INTRODUCTION

Huntington's disease (HD) is an inheritable and autosomal dominant disease, and is caused by an expansion of CAG trinucleotide repeats in exon 1 of the *Huntingtin* (*HTT*) gene.[1] The expanded HTTs are proteolysed and misfolded to form aggregates, and lead to cellular cytotoxicity and neuronal degeneration in the cortex and striatum regions of brains of HD patients.[2–4] Until now, there has been no cure for HD, and physicians can only alleviate clinical symptoms using different treatments, with the result that HD patients suffer unimaginable pain before death.

MicroRNAs (miRNAs) are non-coding RNAs, and their function is to downregulate the translation of target genes, further influencing physiological and pathological conditions in different species. In HD, miRNAs are involved in disease progression and pathological phenotypes,[5,6] suggesting that miRNAs might be potential therapeutical targets in this disease. Based on previous studies, one specific miRNA, miR-196a, has been reported to play roles in the pathogenesis or potential therapy for different neurodegenerative diseases, including spinal and bulbar muscular atrophy, Alzheimer's disease, and HD.[4,7–11] In HD, miR-196a was predicted to modify several biofunctions, such as apoptosis signaling, immune system, cytoskeleton, tissue remodeling, wound repair, etc.[12] Especially, miR-196a has been confirmed to improve neuropathological and behavioral phenotypes in HD, and also has increased neurite outgrowth through enhancing β-tubulin polymerization to provide neuroprotection.[4,13,14] These results suggest that neuronal cytoskeletons or neurite outgrowth are important factors for miR-196a with regard to beneficial functions in HD.

Neurite outgrowth is organized through cytoskeleton arrangement, in particular microtubules and actins, to facilitate neuronal development and regeneration.[15] Microtubules dominantly include α-tubulin and β-tubulin, which polymerize to form cell shape, and further are responsible for axon specification, intracellular trafficking, neuronal migration, etc. The actin structure composes G-actin monomers to polymerize into F-actin, known as actin filament, and forms lamellipodia, filopodia, and stress fibers to process morphogenesis.[16] Especially, actin assembly is necessary for neurite outgrowth at the initial step and dendrite and dendritic spine formation at later stages,[17] further facilitating synaptic functions in neurons.[18] In HD, several reports have shown deficits in neuronal morphology during disease progression,[13,19–23] suggesting that enhancement of the neuronal

Received 8 June 2022; accepted 6 October 2022;
https://doi.org/10.1016/j.omtn.2022.10.002.

[4]These authors contributed equally

Correspondence: Shang-Hsun Yang, Ph.D., Department of Physiology, College of Medicine, National Cheng Kung University, Tainan 70101, Taiwan.
E-mail: syang@mail.ncku.edu.tw

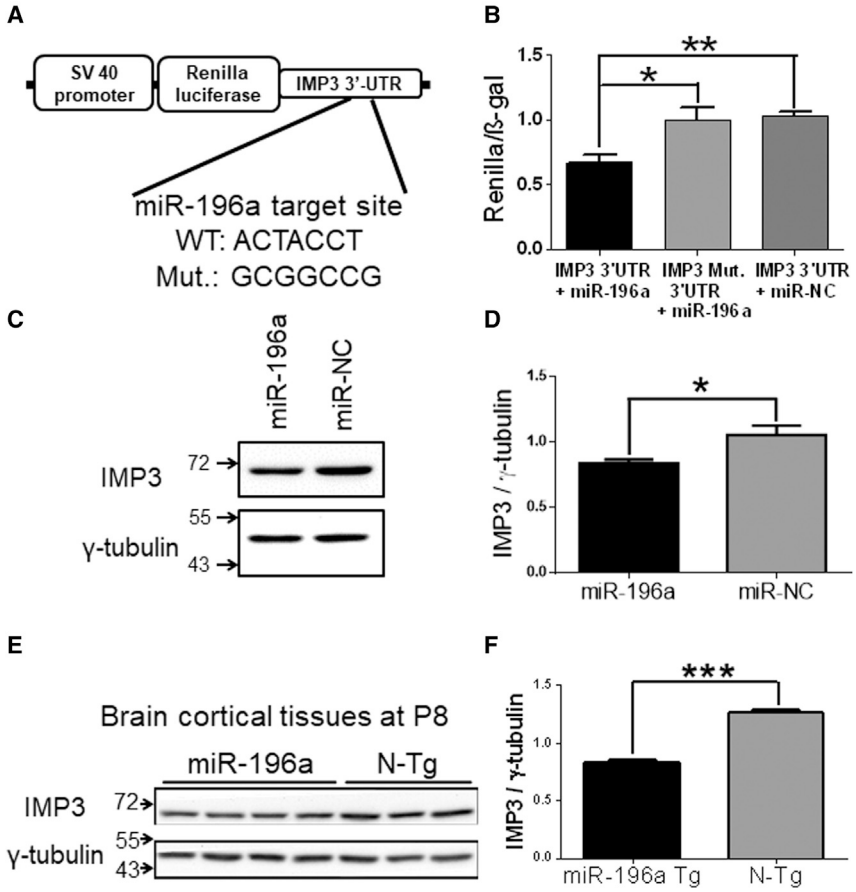

Figure 1. miR-196a directly suppresses the expression of IMP3 *in vitro* and *in vivo*

(A and B) N2a cells were co-transfected with miR-196a and a reporter construct to determine the direct binding of miR-196a on 3′ UTR of IMP3. (A) 3′ UTR of IMP3 with the wild-type (WT) or mutant (Mut.) target site was inserted into the 3′ end of the luciferase gene for the reporter assay. (B) The luciferase reporter assay shows that miR-196a binds to the 3′ UTR of IMP3 to suppress the expression of luciferase activity compared with those of IMP3 mutant 3′ UTR and miR-196a non-relative control (NC) groups. N = 5. N2a cells transfected with miR-196a (C and D) and the brains of miR-196a transgenic mice (E and F) were used to determine the effects of miR-196a on endogenous IMP3. (C) Western blotting shows the expression of IMP3 after the treatments of miR-196a mimics and NC in N2a cells. (D) Quantitation results show the suppression of IMP3 after treatments with miR-196a mimics in N2a cells. N = 3. (E) Western blotting shows the expression of IMP3 in the brains of non-transgenic (N-Tg) and miR-196a transgenic mice. (F) Quantitation results show the lower expression of IMP3 in miR-196a transgenic mice (N = 3 for N-Tg mice; N = 4 for miR-196a mice). *p < 0.05, **p < 0.01, ***p < 0.001.

cytoskeleton is a potential direction to alleviate the neuropathogenesis in these neuronal diseases.

The insulin-like growth factor 2 mRNA binding protein (IGF2BP or IMP) family includes IGF2BP1, IGF2BP2, and IGF2BP3, and all of them contain conserved RNA recognition motifs and hnRNP K homology domains to interact with specific RNAs, such as insulin-like growth factor-II (IGF2).[24–26] IGF2BP3, as known as IMP3, is usually expressed only during fetal development, and abnormal expression of this protein in adulthood often leads to malignant tumorigenesis, especially metastasis.[27,28] Based on previous review articles, IMP3 is involved in actin dynamics, and dynamics of G/F actin equilibrium are highly related to cell adhesion and migration.[29,30] In addition, a *Drosophila* homolog of IMP3, dIMP, has been shown to be a modulator of neuronal differentiation.[31,32] These imply that expression of IMP3 in neurons may influence the cytoskeleton and neuronal morphology to further affect neuronal functions.

In our previous studies, we identified that miR-196a enhances assembly of β-tubulin to improve neurite outgrowth, and further accelerates intracellular transportation, synaptic plasticity, neuronal activity, and learning and memory in different models *in vitro* and *in vivo*.[13] While microtubules and actins are two important cytoskeleton components for neuronal morphology, whether miR-196a could provide neuroprotective functions through actins in HD is still unclear. In this study, we demonstrate the regulatory effects of miR-196a on target genes related to actin dynamics, and further identify the potential neuroprotective mechanisms of miR-196a in HD.

RESULTS

miR-196a directly suppresses the expression of IMP3 to increase neurite outgrowth

Based on previous studies, we have shown that miR-196a increases neurite outgrowth through the increase of β-tubulin polymerization.[13] Since microtubules and microfilaments are two important components of neuronal cytoskeleton, we attempt to demonstrate the role of microfilaments in neurite outgrowth induced by miR-196a. We first screened the predicted targets of miR-196a via the TargetScan website (http://www.targetscan.org/vert_72/), and identified one direct target, IGF2BP3 (as known as IMP3) whose binding site of the 3′ untranslated region (UTR) for miR-196a is highly conserved among different species (Figure S1). According to previous studies, IMP3 has been reported to be involved in actin dynamics during tumorigenesis.[29,30] To examine whether miR-196a directly binds to the 3′ UTR of IMP3, we cloned the 3′ UTR of IMP3 (accession number: NM_023670.3) into a luciferase reporter construct, and mutated the miR-196a target site to examine the binding specificity as well (Figure 1A).[13] These constructs were then cotransfected with miR-196a or non-relative control miRNA (miR-NC) into N2a cells, and direct

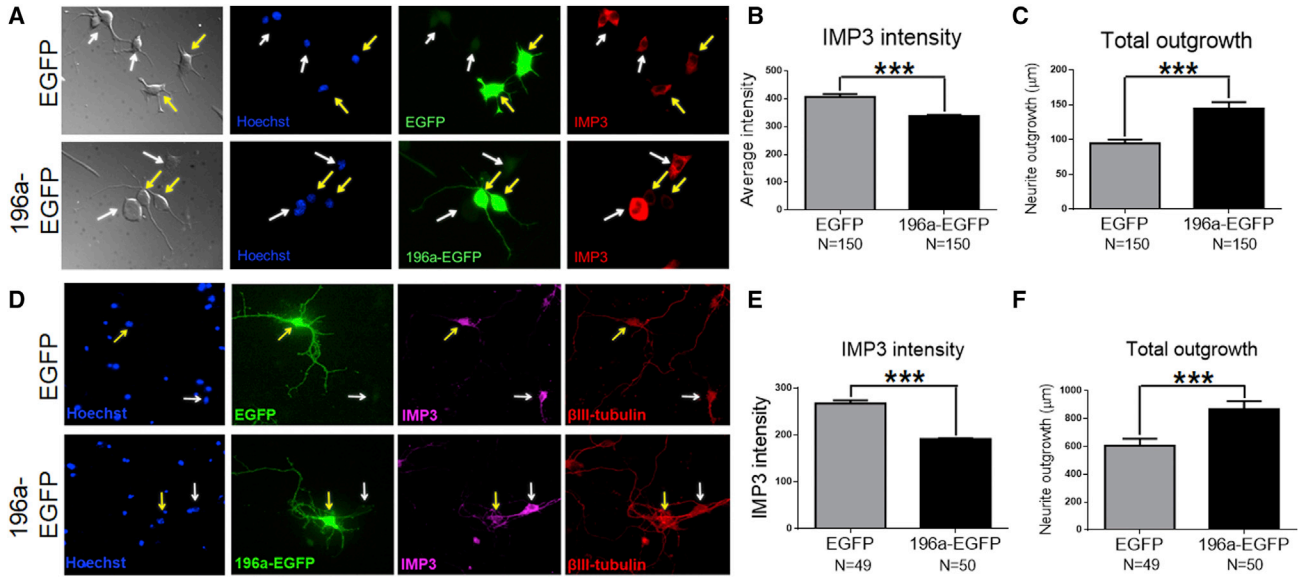

Figure 2. miR-196a suppresses the expression of IMP3 and further increases neurite outgrowth in N2a cells and primary neurons

(A–C) N2a cells were transfected with EGFP or miR-196a-EGFP plasmids, cultured for 48 h, and then subjected to immunostaining using an IMP3 antibody. (A) Representative images show the morphology of transfected cells. Yellow arrows indicate the transfected cells, and white arrows indicate non-transfected cells. Hoechst staining indicates the cell nucleus in blue. Green indicates cells transfected with EGFP or miR-196a-EGFP. Red indicates the expression of IMP3. (B) Quantitation results show the suppression of IMP3 intensity after treatments with miR-196a. (C) Quantitation results show the increase of neurite outgrowth after treatments with miR-196a. (D -F) Primary neurons at 5 days *in vitro* (DIV) were transfected with EGFP or miR-196a-EGFP plasmids, cultured for 48 h, and then subjected to immunostaining using IMP3 and βIII-tubulin antibodies. (D) Representative images show the morphology of transfected cells. Yellow arrows indicate the transfected cells, and white arrows indicate non-transfected cells. Hoechst staining indicates the cell nucleus in blue. Green indicates cells transfected with EGFP or miR-196a-EGFP. Purple indicates the expression of IMP3. Red indicates the expression of βIII-tubulin. (E) Quantitation results show the suppression of IMP3 intensity after treatments with miR-196a. (F) Quantitation results show the increase of neurite outgrowth after treatments with miR-196a. ***$p < 0.001$.

binding of miR-196a with the 3′ UTR of IMP3 was evaluated via the expression of luciferase activity. Based on the luciferase assay, miR-196a suppresses 33.2% ± 11.54% and 35.4% ± 6.79% of luciferase activity compared with those of IMP3 mutant 3′ UTR and NC miRNA control groups, respectively (Figure 1B). We further determined the effects of miR-196a on endogenous IMP3 in N2a cells *in vitro* and miR-196a transgenic mice *in vivo*. As miR-196a was transfected into N2a cells, endogenous IMP3 was significantly reduced by 20.4% ± 7.40% compared with that of miR-NC (Figures 1C and 1D). In miR-196a transgenic mice *in vivo*, we examined brain cortex at 8 days of age because IMP3 does not express in adult stage,[33] showing that miR-196a transgenic mice display 35.0% ± 3.82% lower levels of endogenous IMP3 compared with those of non-transgenic (N-Tg) mice (Figures 1E and 1F). In addition, we also performed immunostaining in N2a cells and primary neurons transfected with miR-196a carrying a green fluorescent protein (GFP) (Figure 2). Under the same staining and exposure conditions, miR-196a suppresses 17.0% ± 2.60% and 28.4% ± 2.66% of the fluorescent intensity of endogenous IMP3, respectively (Figures 2A, 2B, 2D, and 2E), and increases 50.13 ± 10.80 and 263.2 ± 77.29 μm of neurite outgrowth in N2a cells and primary neurons, respectively (Figures 2A, 2C, 2D, and 2F), which is consistent with our previous study.[13] Taking these results together, they suggest that miR-196a directly binds to the 3′ UTR of IMP3 to suppress protein expression *in vitro* and *in vivo*.

IMP3 worsens neurite outgrowth *in vitro* and *in vivo*

Since miR-196a increases neurite outgrowth, we wonder whether IMP3, which relates to cellular microfilaments, affects neurite outgrowth. To examine the role of IMP3 in neurite outgrowth, we constructed an IMP3-Flag plasmid containing IMP3 (accession number: NM_026670.3) under control of a human ubiquitin promoter. After delivering into N2a cells, exogenous IMP3 was overexpressed based on western blotting (Figure S2A). To demonstrate the effects of IMP3 on neurite outgrowth, we transfected IMP3 into N2a cells and primary neurons (Figure 3), and then performed immunostaining to determine neurite outgrowth. In the cells transfected with GFP control plasmids, the morphology of neurite outgrowth was similar between cells transfected with or without GFP (Figures 3A and 3C, top panels). However, as cells were transfected with IMP3, the neurite outgrowth of these cells was decreased by 31.22 ± 5.492 μm in N2a cells (white arrows in Figures 3A, bottom panel, and 3B) and 185.2 ± 46.92 μm in primary neurons (white arrows in Figures 3C, bottom panel, and 3D), respectively. We further generated IMP3 transgenic mice, and showed expression of exogenous IMP3 in the cortex of mouse brains (Figure S2B). However, these IMP3 transgenic founders could not have germline transmission to offspring for unknown reasons. Therefore, we collected brains from two IMP3 transgenic founders, and then performed Golgi staining to stain neurons. In non-transgenic mice, there are more extended axons of pyramidal neurons to the fifth–sixth layers in cortex

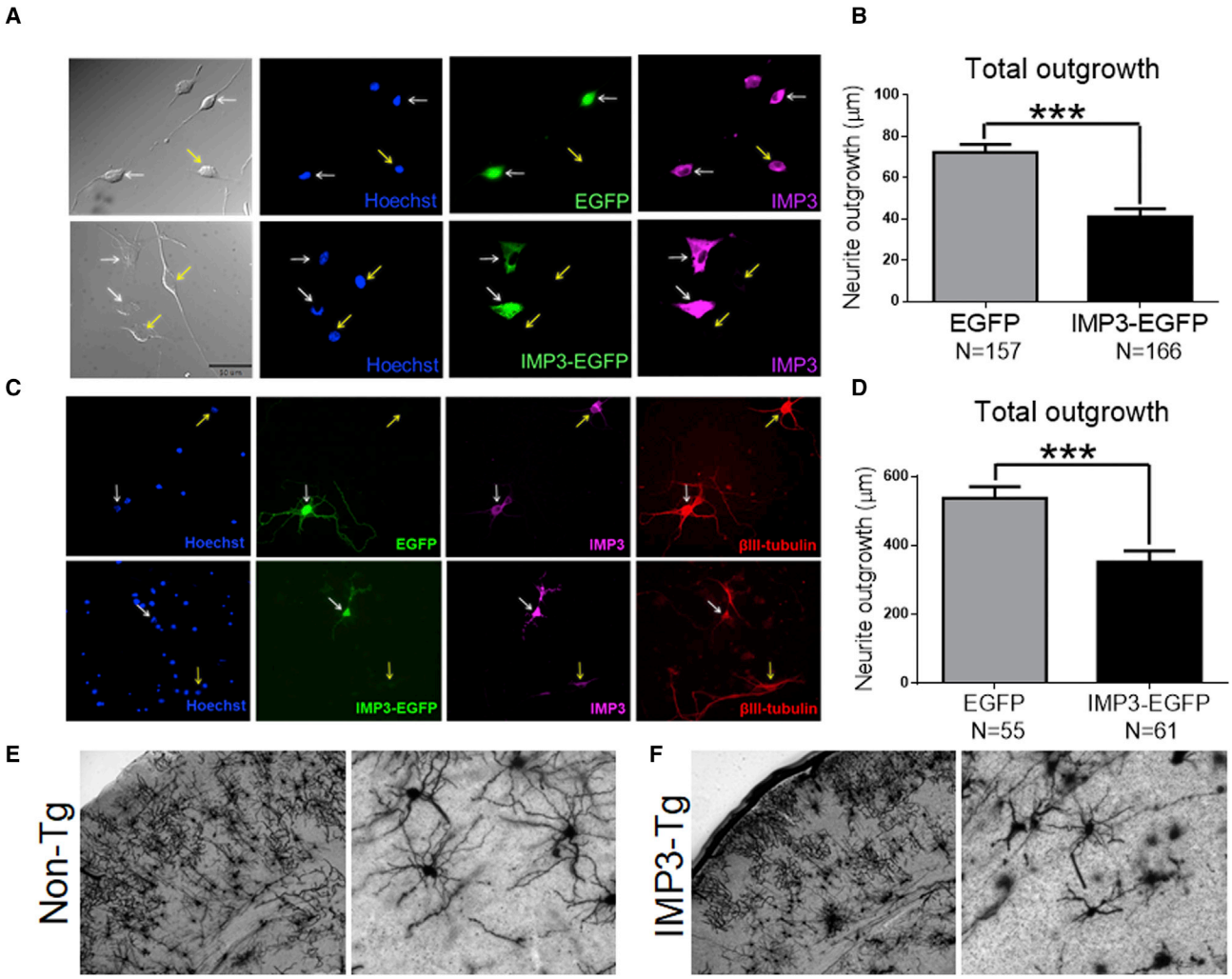

Figure 3. IMP3 significantly worsens neurite outgrowth *in vitro* and *in vivo*

(A and B) N2a cells were transfected with EGFP or IMP3-EGFP plasmids, cultured for 48 h, and then subjected to immunostaining using an IMP3 antibody. (A) Representative images show the morphology of transfected cells. Yellow arrows indicate the non-transfected cells, and white arrows indicate transfected cells. Hoechst staining indicates the cell nucleus in blue. Green indicates cells transfected with EGFP or IMP3-EGFP. Purple indicates the expression of IMP3. (B) Quantitation results show the decrease of neurite outgrowth after treatments with IMP3 in N2a cells. (C and D) Primary neurons at DIV 5 were transfected with EGFP or IMP3-EGFP plasmids, cultured for 48 h, and then subjected to immunostaining using IMP3 and βIII-tubulin antibodies. (C) Representative images show the morphology of transfected cells. White arrows indicate the transfected cells, and yellow arrows indicate non-transfected cells. Hoechst staining indicates the cell nucleus in blue. Green indicates cells transfected with EGFP or IMP3-EGFP. Purple indicates the expression of IMP3. Red indicates the expression of βIII-tubulin. (D) Quantitation results show that IMP3 suppresses neurite outgrowth in primary neurons. (E and F) Golgi staining were performed by using brain samples from non-transgenic (E) and IMP3 transgenic (F) mice at age 2 months. ***$p < 0.001$.

regions (Figure 3E, left panel) compared with those of IMP3 transgenic mice (Figure 3F, left panel). In addition, relatively more neurites were observed in neurons in non-transgenic mice (Figure 3E, right panel) compared with those of IMP3 transgenic mice (Figure 3F, right panel). Taking these results together, they suggest that IMP3 significantly worsens neurite outgrowth *in vitro* and *in vivo*.

miR-196a increases neurite outgrowth through IGF2

Since we hypothesize that miR-196a may increase neurite outgrowth through suppressing the expression of IMP3, we further demonstrate the critical role of IMP3 in this miR-196a regulatory pathway via the blockage of suppressed IMP3. We overexpressed miR-196a and IMP3 together to block this regulation, and then observed the neurite outgrowth in N2a cells. Because miR-196a carries EGFP and IMP3 carries dsRed, we compared the neurite outgrowth of transfected cells overexpressing miR-196a-EGFP with dsRed (Figure 4A, top panel) or with IMP3-DsRed (Figure 4A, bottom panel). As cells overexpress miR-196a with IMP3, IMP3 worsens neurite outgrowth induced by miR-196a by 40.56 ± 7.225 μm (Figure 4B), suggesting the critical

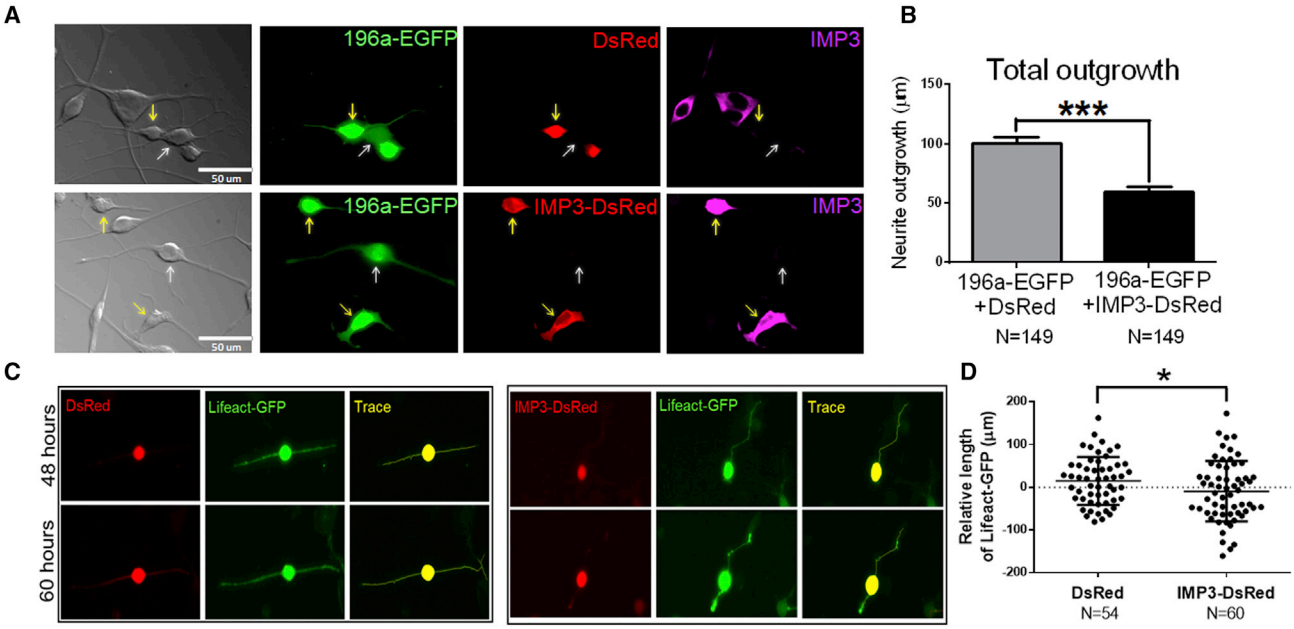

Figure 4. Overexpression of IMP3 disrupts neurite outgrowth induced by miR-196a

(A and B) N2a cells were co-transfected miR-196a-EGFP with dsRed or IMP3-DsRed plasmids, cultured for 48 h, and then subjected to immunostaining using an IMP3 antibody. (A) Representative images show the morphology of transfected cells. Yellow arrows indicate cells co-transfected miR-196a-EGFP with dsRed or IMP3-DsRed, and white arrows indicate cells transfected with miR-196a-EGFP only. Green indicates cells transfected with miR-196a-EGFP. Red indicates cells transfected with dsRed or IMP3-DsRed. Purple indicates the expression of IMP3. (B) Quantitation results show that IMP3-DsRed decreases neurite outgrowth induced by miR-196a-EGFP. (C and D) N2a cells were cotransfected with Lifeact-GFP and with dsRed (C) (left panel) or IMP3-DsRed (C) (right panel) plasmids, and then the length of Lifeact-GFP was traced in same cells at 48 and 60 h after transfection. (C) Representative images show the signals of Lifeact-GFP (green) in cotransfected cells (red) at 48 and 60 h after transfection. Artificial yellow indicates the traced cells and length of Lifeactin-GFP identified by MetaMorph software. (D) Quantitation results show that IMP3-DsRed decreases the relative length of Lifeact-GFP between 48 and 60 h. *$p < 0.05$, ***$p < 0.001$.

role of IMP3 in this miR-196a regulatory pathway for neurite outgrowth.

According to previous studies, IMP3 is involved in actin dynamics,[29,30] which is related to the microfilament of the cytoskeleton. Since we have shown that miR-196a enhances polymerization of neuronal microtubules,[13] another important component of the cytoskeleton, we further demonstrate the effects of IMP3 on actin dynamics. Taking advantage of the fact that Lifeact-GFP, which could trace actin organization and cellular morphology,[34] we cotransfected Lifeact-GFP with IMP3-DsRed or dsRed plasmids into N2a cells, and then traced neurite length in same cells at 48 and 60 h after transfection. As shown in Figures 4C and 4D, the Lifeact-GFP signals in the same cells were determined by the MetaMorph software at different time points (Figure 4C), and overexpression of IMP3-dsRed significantly decreases the length indicated by Lifeact-GFP by 24.08 ± 12.03 μm between 48 and 60 h (Figure 4D). These results suggest that IMP3 worsens the actin dynamics and that miR-196a might increase neurite outgrowth by improving actin polymerization.

miR-196a increases neurite outgrowth by IGF2

To further investigate the downstream target regulated by miR-196a/IMP3, we address IGF2, which may be a potential candidate based on a previous study.[26] Here, we hypothesize that miR-196a further functions through IGF2 to increase neurite outgrowth. We first transfected miR-196a mimics into N2a cells, and then determined the expression level of IGF2 via western blotting. Results show that 11.8% ± 3.99% of IMP3 is suppressed by miR-196a (Figures 5A and 5B, left panel), but 20.60% ± 7.12% of IGF2 is increased compared with those of NC control (Figures 5A and 5B, right panel). We also performed immunostaining, showing that miR-196a increases IGF2 by 102.32% ± 53.89% (Figure S3). In addition, we delivered IMP3 into N2a cells, and then examined the expression of IGF2 by western blotting (Figure 5C). Due to an alternative start site, two exogenous bands were detected, and the results show that IMP3 decreases IGF2 by 15.7% ± 5.36% (Figure 5D). These results suggest that miR-196a decreases IMP3 and increases IGF2 expression. Next, we tried to determine the effects of IGF2 on neurite outgrowth. We transfected IGF2-EGFP into N2a cells, and then observed neuronal morphology (Figure 5E), showing that IGF2 increases total neurite outgrowth by 55.67 ± 9.541 μm compared with that of the EGFP control (Figure 5F). Furthermore, we also examined the critical role of IGF2 in the increase of neurite outgrowth induced by miR-196a. Since miR-196a increases the expression of IGF2 (Figures 5A and 5B), we tried to determine the neurite outgrowth as miR-196a is overexpressed and IGF2 is suppressed simultaneously in N2a cells

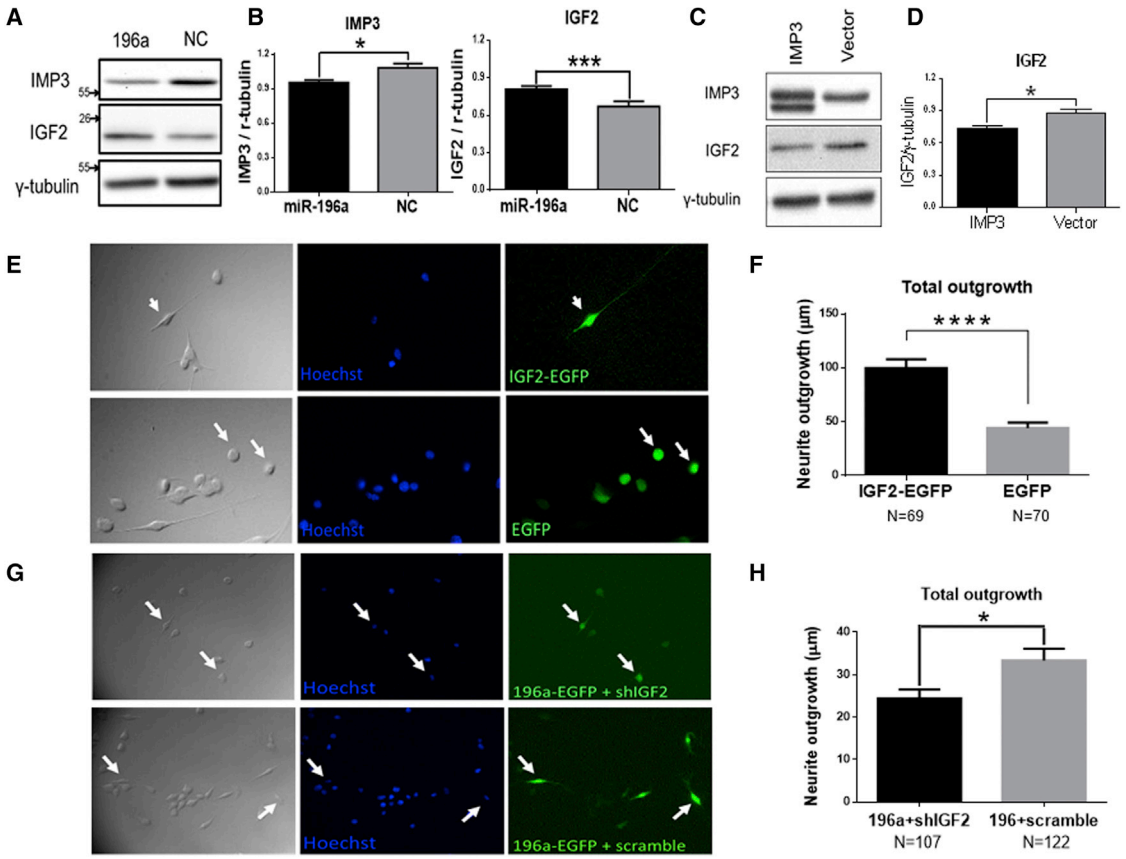

Figure 5. miR-196a increases neurite outgrowth through IGF2 in N2a cells

N2a cells were transfected with different plasmids, cultured for 48 h, and then subjected to western blotting and fluorescent image analyses. (A) Western blotting shows the expression of IMP3 and IGF2 after treatments with miR-196a mimics and NC in N2a cells. (B) Quantitation results show the decrease of IMP3 (left panel) and increase of IGF2 (right panel) in the miR-196a group compared with those of the NC group in N2a cells. N = 5. (C) Western blotting shows the expression of IMP3 and IGF2 after treatment with IMP3 in N2a cells. (D) Quantitation results from (C) show that IMP3 decreases the expression of IGF2 compared with those of the vector control group in N2a cells. N = 4. (E) Representative images show the morphology of cells transfected with IGF2-EGFP or EGFP (white arrows). Hoechst staining indicates the cell nucleus in blue. Green indicates cells transfected with IGF2-EGFP or EGFP. (F) Quantitation results from (E) show that IGF2 increases neurite outgrowth in N2a cells. (G) Representative images show the morphology of cells transfected miR-196a-EGFP with shIGF2 or scramble (white arrows). Hoechst staining indicates the cell nucleus in blue. Green indicates cells transfected miR-196a-EGFP with shIGF2 or scramble. (H) Quantitation results from (G) show that downregulation of IGF2 decreases the effects of miR-196a on neurite outgrowth in N2a cells. *p < 0.05, ***p < 0.001, ****p < 0.0001.

(Figure 5G). As shown in Figure 5G, knockdown of IGF2 via shIGF2 shortens neurite outgrowth induced by miR-196a by 8.962 ± 3.556 μm compared with that of the sh-scramble group (Figure 5H). Taking these results together, they suggest that miR-196a increases neurite outgrowth by suppressing IMP3 and then overexpressing IGF2.

IGF2 increases numbers of filopodia and active forms of Cdc42

Based on above results in Figure 4, we have figured out the role of microfilaments, especially actin dynamics, regulated by the miR-196a/IMP3 pathway. Here, we further demonstrate the effects of IGF2 on microfilaments since we have shown that miR-196a increases neurite outgrowth through IGF2 (Figure 5). We transfected IGF2-EGFP into N2a cells, and then stained these cells with Phalloidin, which binds to F-actin specifically. Because filopodia are an important cellular structure dominantly formed by actin polymerization, we quantitated filopodia numbers and average length in these transfected cells using MATLAB software from Perkins Lab.[35] In Figure 6A, we defined the filopodia upon the software, and the results show more detected signals of filopodia in IGF2-EGFP cells compared with those in EGFP cells. We quantitated these signals, and found that there are significantly more numbers of filopodia (4.789 ± 1.428) in IGF2-EGFP cells (Figure 6B, top panel). However, the average lengths of filopodia are similar between IGF2-EGFP and control groups (Figure 6B, bottom panel). Furthermore, because Cdc42 is responsible for the regulation of actin cytoskeleton to form filopodia,[36] we further determined the active form of Cdc42 via a p21-activated kinase 1 (PAK)-p21 binding domain (PBD) pull-down assay.[37] As shown in Figures 6C and 6D, the active form of Cdc42 is significantly higher in IGF2 cells (63.4% ± 20.01%) compared with that in EGFP cells.

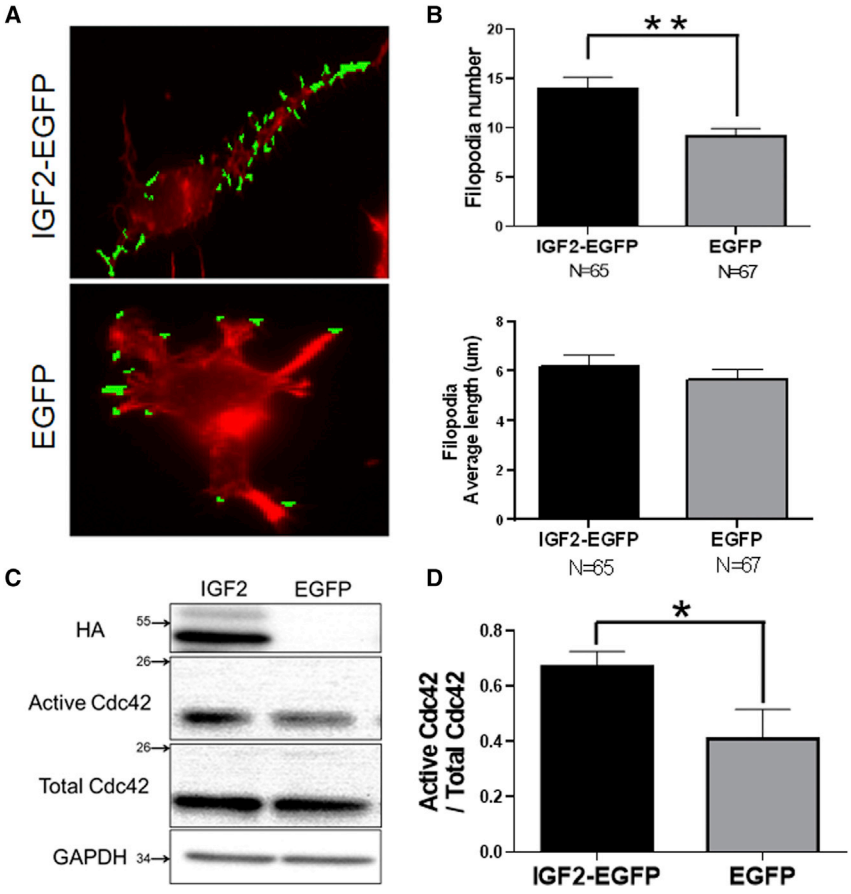

Figure 6. IGF2 increases filopodia numbers and active forms of Cdc42

N2a cells were transfected with IGF2-EGFP or EGFP plasmids, cultured for 48 h, and subjected to determination of the formation of filopodia and activity of Cdc42. (A) Representative images show the detection of filopodia via MATLAB software in transfected cells. Green indicates filopodia, and red indicates IGF2 transfected cells. (B) Quantitation results from (A) show that IGF2 increases filopodia numbers, but not filopodia average length in N2a cells. (C) Western blotting shows the expression of active Cdc42 and total Cdc42 after treatments with IGF2. The EGFP plasmid was used as a control. The HA antibody detects the expression of exogenous IGF2 due to the exogenous IGF2 fused with the HA tag. (D) Quantitation results from (C) show that IGF2 increases the active form of Cdc42 in N2a cells. N = 3. *p < 0.05, **p < 0.01.

These results suggest that miR-196a upregulates IGF2 to activate Cdc42, further enhancing actin filopodia to increase neurite outgrowth.

miR-196a increases neurite outgrowth through IGF2 in HD

Since miR-196a provides neuroprotective functions in HD, we further demonstrate the above mechanisms under HD conditions. Here, we used primary neurons isolated from R6/2 HD transgenic mice, which is a well-defined HD transgenic mouse model,[13] as an HD model. We first confirm the neurite outgrowth of primary neurons from R6/2 transgenic mice is significantly decreased by 177.5 ± 31.38 μm compared with that of non-transgenic mice (Figures 7A and 7B left panel). As we delivered miR-196a into R6/2 primary neurons, miR-196a significantly increased neurite outgrowth by 56.98 ± 23.48 μm (Figures 7A and 7B right panel). Moreover, IGF2 also increases neurite outgrowth by 36.81 ± 14.68 μm in R6/2 primary neurons (Figures 7C and 7D). These results suggest the beneficial roles of miR-196a and IGF2 for the neurite outgrowth in HD. We further examine the critical role of IGF2 in neurite outgrowth induced by miR-196a in R6/2 HD primary neurons. Two models of primary neurons were used, including primary neurons from R6/2 HD transgenic mice (Figure 7E) and miR-196a-R6/2 double-transgenic mice (Figure 7G). First, we delivered miR-196a-EFGP with shIGF2-dsRed or control plasmids into R6/2 HD primary neurons, and then quantitated the neurite outgrowth, showing that shIGF2 significantly suppresses neurite outgrowth induced by miR-196a in HD primary neurons by 69.12 ± 25.40 μm (Figures 7E and 7F). In addition, we transfected shIGF2-dsRed into primary neurons of miR-196a-R6/2 double-transgenic mice, and showed that shIGF2 significantly suppresses neurite outgrowth in miR-196a-R6/2 double-transgenic mice by 131.9 ± 16.44 μm as well (Figures 7G and 7H). These results support not only the beneficial effects of miR-196a and IGF2 on neurite outgrowth in HD but also the critical role of IGF2 for neurite outgrowth increased by miR-196a in R6/2 HD primary neurons.

Higher IMP3 or lower IGF2 increases HTT aggregates

Finally, we examined the expression profiling of IMP3 and IGF2 in different HD models *in vivo* and *in silico*. We collected brain tissues from R6/2 HD transgenic and non-transgenic mice at age 3 months, which were then subjected to western blotting. As shown in Figures 8A and 8B, R6/2 transgenic mice display aggregated HTT upon mEM48 signals, and also show higher expression of IMP3 and lower expression of IGF2 (12.15% ± 5.24%) in brains. We further analyzed one set of Gene Expression Omnibus (GEO) database (GSE1767), which is the gene expression profiling from HD and control blood samples.[38] We extracted raw data of IMP3 (Figure 8C) and IGF2 (Figure 8E) from this GEO set, and performed statistical analyses. In HD patients, the expressions of IMP3 are significantly higher (92.77% ± 13.88%) (Figure 8D) and the expressions of IGF2 are significantly lower (51.84% ± 9.08%) (Figure 8F) in HD patients than those of controls. We further determined the role of IMP3 and IGF2 toward mutant HTT (mHTT) aggregates in HD. We transfected *IMP3* and *shIGF2* with *mHTT* into N2a cells, and then detected the mHTT by western blotting (Figures 8G and 8I). Results showed that higher expression of IMP3 or lower expression of IGF2 increases

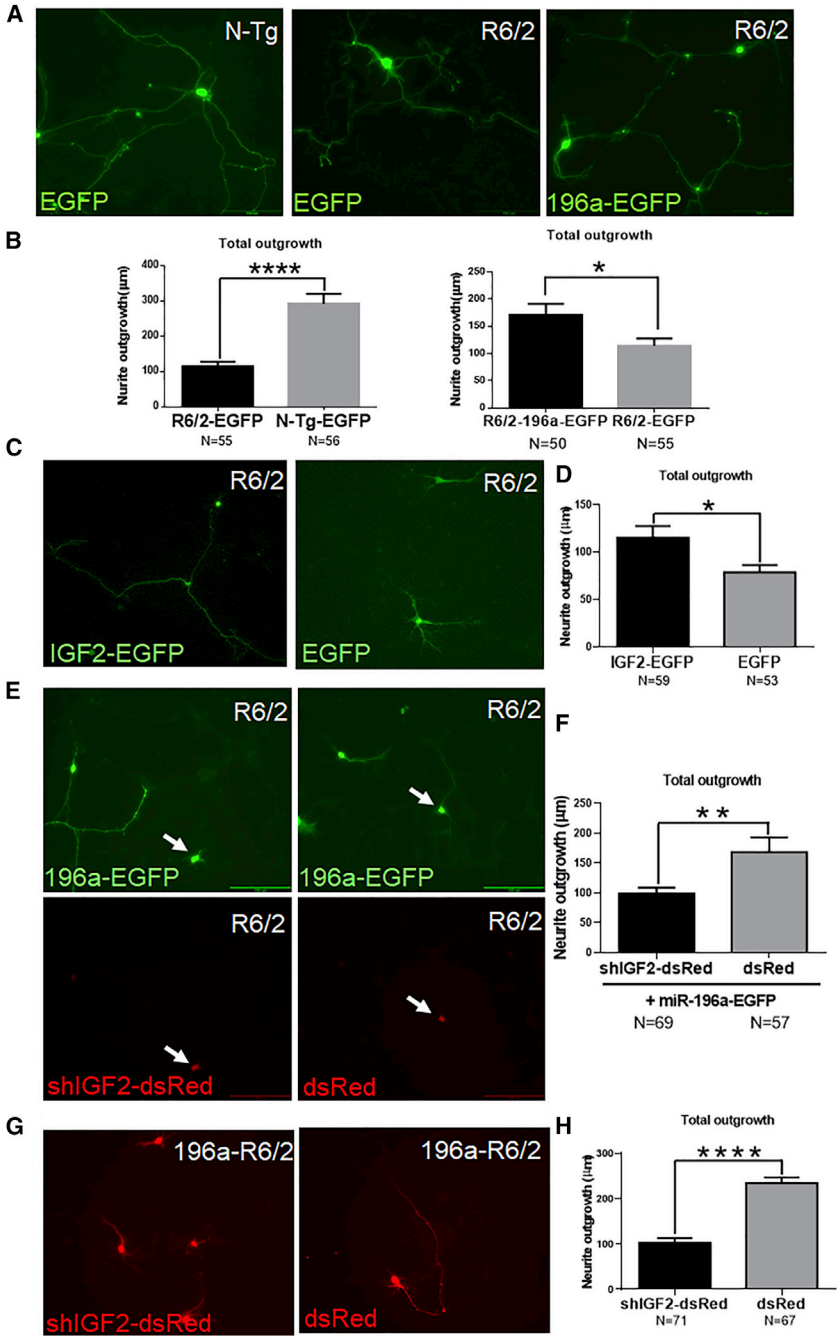

Figure 7. miR-196a increases neurite outgrowth through IGF2 in HD cells

(A–H) Primary neurons from R6/2 transgenic mice were transfected with different plasmids at DIV 5, cultured for 96 h, and then subjected to determination of neurite outgrowth. (A) Representative images show the morphology of primary neurons transfected with EGFP or miR-196a-EGFP (196a-EGFP) plasmids. Primary neurons were from non-transgenic mice (N-Tg, left panel) and R6/2 transgenic mice (middle and right panels). (B) Quantitation results from (A) show R6/2 transgenic mice display significantly shorter neurite outgrowth compared with that of N-Tg mice (left panel). In addition, miR-196a-EGFP increases neurite outgrowth compared with that of the EGFP control in HD primary neurons (right panel). (C) Representative images show the morphology of R6/2 primary neurons transfected with IGF2-EGFP (left panel) or EGFP (right panel) plasmids. (D) Quantitation results from (C) show IGF2-EGFP increases neurite outgrowth compared with that of the EGFP control. (E) Representative images show the morphology of R6/2 primary neurons transfected miR-196a-EFGP with shIGF2-dsRed (top panel) or dsRed (bottom panel) plasmids. Arrows indicate the cotransfected cells. (F) Quantitation results from (E) show that shIGF2-dsRed decreases neurite outgrowth induced by miR-196a-EGFP. (G and H) Primary neurons from miR-196a-R6/2 double-transgenic mice were transfected with shIGF2-dsRed or dsRed. (G) Representative images show the morphology of miR-196a-R6/2 primary neurons transfected with shIGF2-dsRed (left panel) or dsRed (right panel) plasmids. (H) Quantitation results from (G) show that shIGF2-dsRed decreases neurite outgrowth compared with that of dsRed control. *$p < 0.05$, **$p < 0.01$, ****$p < 0.0001$.

mHTT aggregates (49.37% ± 6.43%, Figure 8H; and 44.42% ± 10.26%, Figure 8J, respectively). These results not only show the importance of IMP3 and IGF2 in HD *in vivo*, but also imply that IMP3 and IGF2 may also be involved in the formation or degradation of mHTT aggregates.

DISCUSSION

HD is a terrible neurodegenerative disease with no cure. Thus, it is urgent to understand the detailed mechanisms of disease progression to further provide therapeutical directions for this disease. Based on our series studies, we have shown that miR-196a provides neuroprotective functions against HD through different mechanisms, including increase of neurite outgrowth.[12–14] In this study, we further demonstrated the effects of miR-196a on actin microfilaments and identified the cellular mechanisms through directly suppressing IMP3 and upregulating IGF2 in different models. Combined with our previous study,[13] we show that miR-196a enhances the polymerization of microtubules and microfilaments to benefit the neuronal cytoskeleton, further offering neuroprotective effects against HD.[13,14]

Microfilaments, microtubules, and intermediate filaments are three important cytoskeleton components in neuronal cells, and the positive interaction of these components could reveal physiological functions, such as intracellular transport and synaptic plasticity, in neurons.[39] In neurodegenerative diseases, the neuronal cytoskeleton is disrupted, resulting in degeneration and death of neurons.[40] Thus,

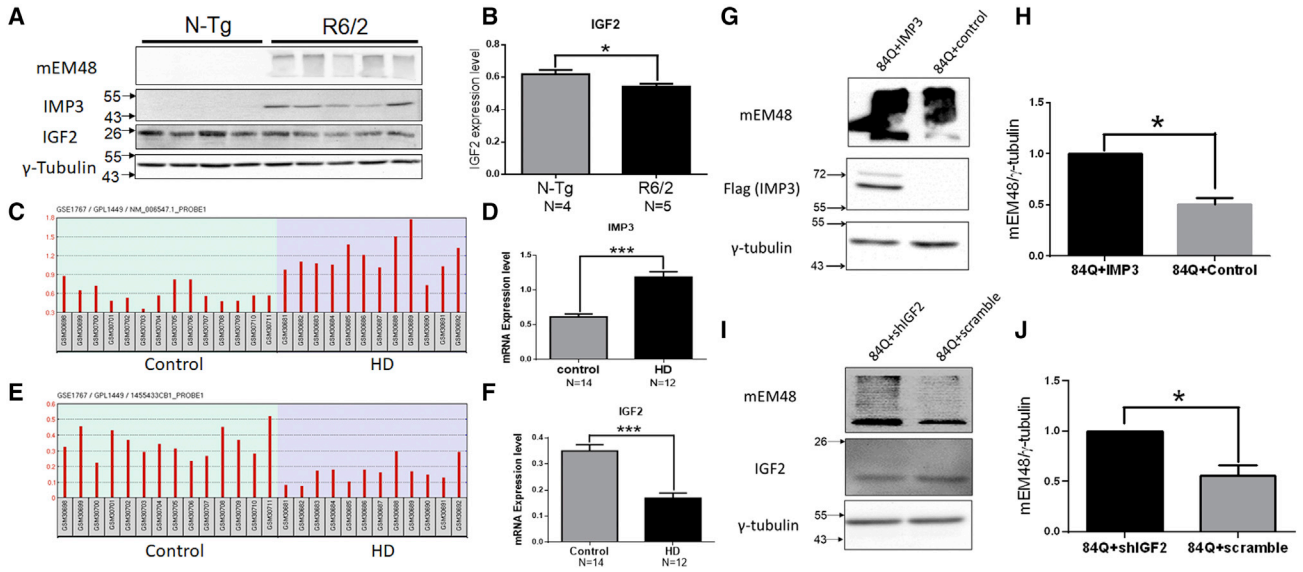

Figure 8. Higher IMP3 or lower IGF2 increases HTT aggregates

(A and B) Brain tissues of R6/2 transgenic and non-transgenic mice at age 3 months were collected, and then subjected to western blotting. (A) Western blotting shows the expression of mHTT (mEM48), IMP3, and IGF2 in non-transgenic (N-Tg) and R6/2 transgenic mice. (B) Quantitation results from (A) show significantly lower expression of IGF2 in R6/2 transgenic mice. (C–F) *In silico* analyses were performed based on GSE1767 from the GEO database. (C) Raw expression level of IMP3 in HD patients and controls was downloaded from GSE1767. (D) Quantitation results from (C) show significantly higher expression of IMP3 in HD patients. (E) Raw expression levels of IGF2 in HD patients and controls were downloaded from GSE1767. (F) Quantitation results from (E) show significantly lower expression of IGF2 in HD patients. (G–J) N2a cells were transfected mHTT-84Q with IMP3 or shIGF2, cultured for 48 h, and then subjected to western blotting. (G) Western blotting shows the expression of mHTT after the transfection of mHTT-84Q with IMP3 or control plasmids. The mEM48 antibody is used for detection of mHTT. The flag antibody is used for detection of exogenous IMP3. γ-Tubulin is used as an internal control. (H) Quantitation results from (G) show that IMP3 increases the expression of mEM48 compared with that of control. (N = 3). (I) Western blotting shows the expression of mHTT after transfection of mHTT-84Q with shIGF2 or control plasmids. (J) Quantitation results from (I) shows that shIGF2 increases the expression of mEM48 compared with that of control. N = 4. *$p < 0.05$, ***$p < 0.001$.

enhancement of the neuronal cytoskeleton is considered as a potential therapy against neurodegenerative diseases, and a number of researchers are focusing on this direction.[41–43] Based on our previous study, we showed that miR-196a increases neurite outgrowth by accelerating the assembly of β-tubulin.[13] Since neurite outgrowth is formed by polymerized microtubules and microfilament-rich growth cones,[39,44,45] this study further supports the importance of actin microfilaments for neurite outgrowth in the neuroprotective mechanism of miR-196a. Because actin cytoskeleton is responsible for filopodia formation, neuronal migration, synaptic functions, axonal development, etc.,[44] our series data support miR-196a offers several beneficial functions related to actin cytoskeleton in neurons. Similar mechanisms are echoed by studies in the field of cancer research,[46,47] strongly supporting the important effects of miR-196a on neuronal morphology.

IMP3, one of miR-196a target genes, dominantly expresses during embryogenesis, and abnormal overexpression has been widely demonstrated in cancer biology, showing IMP3 plays a malignant role during tumor progression.[27,28] However, there are relatively few studies addressing on central nervous system. One study shows higher expression of IMP3 inhibits neuronal differentiation in neuron-like cells,[33] suggesting the worse effects of IMP3 after mid-embryonic stage. In this study, we did not observe the expression of IMP3 in brains of N-Tg mice at adult stage; however, higher expression of IMP3 was observed in HD mice with the same age (Figure 8A). In addition, we observed higher expression level of IMP3 worsens neurite outgrowth *in vitro* and *in vivo* (Figure 3), and IMP3 is expressed higher in HD transgenic mice and patients (Figure 8), indicating the ill role of IMP3 for neurite outgrowth in HD. However, how mutant HTT induces higher expression of IMP3 is still unknown, and further experiments should be conducted to examine this mechanism. In addition, IMP3 is a mRNA binding protein, and regulates gene expression through binding to target mRNAs in cytoplasm. IGF2 is one of IMP3 target mRNAs, but the IMP3 regulation on IGF2 is still contradictory.[26] In our study, we show higher expression of IMP3 leads to lower expression of IGF2 in different neuronal models (Figures 5 and 8), suggesting IMP3 negatively regulates IGF2 expression in these models. This result is not consistent to the expression profiling in most of cancer studies,[48,49] but is similar to the studies related to embryogenesis.[33,50] These imply that the different regulatory pathways of IMP3 on IGF2 in different tissues or conditions, and the detailed regulatory mechanism in HD is deserved for further studies.

In this study, we show IMP3 and IGF2 affect the actin dynamics and structures to influence neurite outgrowth (Figures 4 and 6). Since

IMP3 has been reported to bind to not only IGF2 but also actin mRNAs,[30,51] these previous studies further support the critical roles of IMP3 and IGF2 in miR-196a regulatory mechanism toward neurite outgrowth. In addition, we show IGF2 activates Cdc42 (Figure 6), which is one of key proteins regulating actin cytoskeleton to form filopodia. Therefore, the activity of other regulatory proteins related to cellular actin dynamics, such as Rac1 and RhoA,[52] should also be further considered to address to this regulatory network. Cdc42 has been shown to stimulate neurite outgrowth by the formation of filopodia,[53] thus supporting the enhancement of actin dynamics is a dominant mechanism for neurite outgrowth induced by miR-196a. Since the actin cytoskeleton is also responsible for cellular migration, synaptic connection, and axonal polarization, our results further support the neuroprotective roles of miR-196a against HD.

IGF2 has been shown to provide neuroprotective functions in different neuronal diseases. For example, IGF2 has induced Akt phosphorylation, glycogen synthase kinase-3β phosphorylation, and β-catenin levels against toxic aggregations in amyotrophic lateral sclerosis,[54] and also has reduced β-amyloid plaques in the hippocampus to improve memory in the mouse model of Alzheimer's disease.[55] These results suggest that IGF2 might have a potential role in the degradation of disease-causing aggregates. Based on our previous studies, we report that miR-196a significantly decreases the expression of aggregated mHTT.[4,14] In this study, we further show that higher expression of IMP3 or lower expression of IGF2 increases mHTT aggregates (Figures 8G–8J), suggesting that miR-196a/IMP3/IGF2 is a potential pathway to degrade aggregated proteins. However, the related regulation regarding protein degradation systems still needs to be clarified. Since miR-196a has approximately 322 predicted targets, based on the miRSystem website,[56] we also found several targets that might be involved in protein degradation systems, such as GABA(A) receptor-associated protein, Baculoviral IAP repeat containing 6, Mitogen-activated protein kinase kinase kinase 1, and TNF receptor-associated factor 6. Because aggregation of disease-causing proteins is also a common feature among different neurodegenerative diseases, it would be interesting to further demonstrate the regulatory mechanisms of miR-196a functioning on protein degradation in future.

In conclusion, we provide evidence that miR-196a increases neurite outgrowth through microfilament polymerization in HD, and that the working mechanism functions by directly suppressing IMP3 and upregulating IGF2. Taking our series studies together, they support that miR-196a enhances polymerization of both microtubules and microfilaments to benefit the neuronal cytoskeleton, and further offers neuroprotection against HD. We have not only identified the related mechanisms but also provide a potential insight toward the therapy of HD.

MATERIALS AND METHODS

DNA constructions

The DNA constructs used in this study include EGFP, miR-196a-EGFP, IMP3-Flag, IMP3-EGFP, IMP3 3′ UTR, IGF2-EGFP, and shIGF2-dsRed. EGFP contains an *enhanced green fluorescence protein (EGFP)* gene under control of a human ubiquitin promoter. miR-196a-EGFP contains a precursor *hsa-miR-196a-2* (accession number: MI0000279) under control of a human ubiquitin promoter and an EGFP gene for cellular detection. IMP3-Flag contains coding sequence of *insulin-like growth factor 2 mRNA binding protein 3 gene* (also known as IGF2BP3 or IMP3; accession number: NM_026670.3) flanking a *FLAG* tag at the 3′ end under control of a human ubiquitin promoter. The IMP3-EGFP construct contains the above IMP3-Flag construct with an EGFP reporter gene under control of a human ubiquitin promoter. All of the above constructs are cloned into a lentiviral vector (Addgene plasmid: no. 14883). Moreover, an IMP3 3′ UTR construct (PIS2-IMP3 3′ UTR) for a luciferase reporter assay contains 3′UTR of IMP3 (accession number: NM_026670.3) flanking the 3′ end of a *luciferase* reporter gene driven by an SV40 promoter in a PIS2 vector (Addgene plasmid: no. 12177). The IGF2-EGFP construct contains insulin-like growth factor 2 gene (accession number: NM_000612.6) with HA and Flag tags at the 3′ end with an EGFP reporter gene under control of a cytomegalovirus (CMV) promoter. The shIGF2-dsRed contains the shRNA against *IGF2* gene (shIGF2) under the control of a U6 promoter with a red fluorescence reporter gene (dsRed), and targets on the GTGGGCA AGTTCTTCCAATAT of IGF2 sequence.

Cell culture, transfection, and differentiation

N2a mouse neuroblastoma cells and primary cortical neurons were used in this study. N2a cells were cultured in MEM (Invitrogen) medium with 10% fetal bovine serum (Hyclone) and 1X Penicillin-Streptomycin (Invitrogen). To transfect and differentiate N2a cells, lipofectamine 2000 (Invitrogen) was used to deliver different constructs, and differentiation was then performed using 10 μM retinoic acid (Sigma) and 2% fetal bovine serum in culture medium for 48 h. For primary neurons, primary cortical neurons were established with the approval by the Institutional Animal Care and Use Committee at National Cheng Kung University, Taiwan. All protocols and methods for animal experiments were supervised with the relevant guidelines and regulations. Simply, cortex tissues from mouse fetuses were collected at 17.5–18.5 days postcoitum, and then digested with 0.05% Trypsin-EDTA (Gibco) to obtain mixed brain cells. These cells were maintained in Neurobasal Medium (Gibco) with 1X B27 (Gibco) and 2 mM L-glutamine (Gibco) to increase neuronal population. To transfect primary neurons, the above cells were cultured for 5 days, and then transfected with different DNA constructs using Lipofectamine 2000 (Invitrogen). Transfected cells were cultured for an additional 2 days (7 days *in vitro*), and neurite outgrowth of these primary neurons was evaluated.

Luciferase reporter assay

The binding activity of miR-196a on 3′ UTR of IMP3 was assessed using a luciferase reporter assay. Simply, the PIS2-IMP3 3′ UTR and CMV-β-gal constructs were cotransfected with miR-196a or miR NC mimics in N2a cells for 48 h, and these transfected cells were analyzed using the Dual-Luciferase Reporter Assay System (Promega). β-Galactosidase activity produced from the CMV-β-gal construct was concurrently used as an internal control for

transfection efficiency. The suppression ability of miR-196a on IMP3 was evaluated by determining luciferase activity normalized by β-galactosidase activity.

Neurite outgrowth

Neurite outgrowth was evaluated in N2a cells and primary cortical neurons.[13] Simply, neurite outgrowth was observed using transfected EGFP markers, and fluorescent images were captured using a DM2500 fluorescent microscope (Leica). The Neurite Outgrowth Application Module supported by MetaMorph software (Molecular Devices) was used to detect cells and quantitate total neurite outgrowth length (Figure S4). At least five regions of interest were selected for analyses, and cells with neurite outgrowth length of at least twice the length of the cell body were used for statistical analyses. Total neurite outgrowth is defined as the total length of skeletonized outgrowth (corrected for diagonal lengths) associated with the cell.

Transgenic mice

Three transgenic mouse lines were used in this study, including miR-196a, IMP3, and R6/2 HD transgenic mice. The animal protocol of this study was approved by the Institutional Animal Care and Use Committee at National Cheng Kung University, Taiwan. MiR-196a transgenic mice carry the precursor hsa-*miR-196a-2* sequence (accession number: MI0000279) driven by a human ubiquitin promoter.[13,14,57] These mice were genotyped via PCR using forward primer GAGGCGTCAGTTTCTTTGGTC and reverse primer TAG CGTAAAAGGAGCAACATAGT to detect the 465 bp amplicon. IMP3 transgenic mice generated via lentiviral transgenesis[57] carry the *IMP3* gene (accession number: NM_026670.3) driven by a human ubiquitin promoter. These transgenic mice were genotyped by PCR using forward primer GAGGCGTCAGTTTCTTTGGTC and reverse primer CTCTGCCGTTTAGGGACCGA to detect the 490 bp amplicon. R6/2 HD transgenic mice carry truncated exon1 of *HTT* gene with expanded polyQ under control of an *HTT* promoter.[58] R6/2 transgenic mice were genotyped using forward primer GGCGAC CCTGGAAAAGCTGA and reverse primer TGAGGAAGCTG AGGAGGCGG to detect approximately 700–800 bp amplicons based on various CAG repeat numbers.

Western blotting analysis

Raw proteins from cells or brains were extracted using RIPA lysis and extraction buffer (Thermo Scientific), and these proteins were then subjected to sodium dodecyl sulfate-polyacrylamide gel electrophoresis (Bio-Rad). The proteins on gels were transferred onto PVDF membranes (Bio-Rad), and then subjected to western blotting. The blotted membranes were blocked in 5% skimmed milk, and hybridized with the primary antibodies. The antibodies used in this study included IMP3 (Abcam; 1:1,000 dilution), Flag-M2 (Sigma; 1:2,000 dilution), mEM48 (Sigma; 1:100 dilution), IGF2 (Abcam; 1:1,000 dilution), and γ-tubulin (Sigma; 1:10,000 dilution). Then, the membranes were hybridized with the secondary peroxidase-conjugated antibodies (Jackson ImmunoResearch Laboratories), and protein expression levels were detected using an Amersham ECL kit (PerkinElmer) using an automatic gel imaging system (ChampGel). The quantitation of protein expression was conducted using ImageJ software (NIH).

Immunohistochemical staining

Experimental cells were fixed using 4% paraformaldehyde, and blocked in blocking buffer (0.2% Triton X-100, 3 mM sodium azide, 0.1% saponin, 2% BSA, 5% donkey serum, in phosphate-buffered saline buffer) for 1 h. The cells were incubated with primary antibodies, including IMP3 (Abcam; 1:100 dilution) and βIII-tubulin (Millipore; 1:1,000 dilution) antibodies, at 4°C overnight. After washing with phosphate-buffered saline buffer, the cells were then incubated with secondary antibodies conjugated with Alexa Fluor 488, 594, or 647 (Invitrogen) for 2 h. The nuclei of the cells were stained using 1 μg/mL Hoeschst 33342 (Sigma), and then fluorescence images were captured using a DM2500 fluorescent microscope (Leica). The intensity of IMP3 was determined using MetaMorph software (Molecular Devices).

Golgi stain

FD Rapid GolgiStain Kit (FD Neurotechnologies) was used to determine the neurite outgrowth *in vivo*. Simply, mouse brains were stained in mixed solution A and solution B at room temperature for 10 days, and then transferred to solution C for 3 days. Treated brains were cryosectioned at 140 μm thickness, and then exposed in the staining solution with solution D, solution E, and double Milli-Q water (1:1:2 mix) for 10 min. These brain sections were then dehydrated in 50%, 75%, and 95% ethanol, respectively, and then fixed on slides. To analyze the neurite outgrowth, the images of brain slides were captured every 2 μm along the z axis, and these images were packed into 2D images using MetaMorph software (Molecular Devices). These images of neurite outgrowth were then statistically quantitated by NeuronJ (NIH).[13]

Actin polymerization

Lifeact-GFP plasmid was used to examine the actin polymerization.[34] N2a cells were co-transfected with Lifeact-GFP and IMP3-dsRed plasmids, and then cultured for 48 h. IMP3-dsRed cells with GFP signals were randomly chosen, and the positions of these cells were located via MetaMorph software (Molecular Devices) under the automatic plate of a DMi8 inverted microscope (Leica). The images of GFP signals were captured to trace the actin polymerization. These cells were cultured for 12 h (60 h after transfection), and the GFP signals were again captured in the cells. The relative length of Lifeact-GFP was determined by subtraction of the GFP length between 60 and 48 h.

Analysis of filopodia

The transfected N2a cells were fixed using 4% paraformaldehyde, and then stained with 1X CytoPainter Phalloidin-iFluor 594 Reagent (Abcam) for 30 min. The Phalloidin fluorescent images were captured, and then subjected to analyses of filopodia using the MATLAB with an image process tool software. The input code was quoted

from Perkins Lab,[35] and the distance calibration was performed for correction (μm/pixel). The numbers of filopodia and average lengths were then detected and counted using the software, and the results were subjected to statistical analyses.

Pull-down assay

Active forms of Cdc42 were analyzed using the Cdc42 Pull-Down Activation Assay Biochem Kit (Cytoskeleton). Simply, raw proteins from transfected cells were mixed with PAK-PBD beads to pull down the active form of Cdc42 proteins, and then the bound-proteins were purified and eluted out for western blotting using a Cdc42 antibody. Raw proteins were used to detect the total Cdc42, and the expression levels of active Cdc42 were normalized by total Cdc42.

Bioinformatic analysis

The binding sites of miR-196a on IMP3 3′ UTR was predicted via TargetScan 6.2 (http://www.targetscan.org/). The expression profiling of IMP3 in HD patients and controls was analyzed through the GEO database (https://www.ncbi.nlm.nih.gov/geo/). The accession number used in this study is GSE1767.[38]

Statistical analysis

Data are represented as mean ± standard error of mean (SEM). Student's t test was used to compare differences between two different groups. In some occasions, differences among different groups were analyzed using one-way analysis of variance via a commercial statistical software (GraphPad Prism 4.02; GraphPad Software, San Diego, CA). Tukey's procedure was used to test differences among different groups. Statistical significance was set at $p < 0.05$.

Data availability statement

All data generated or analyzed during this study are included in this article and its supplementary files.

SUPPLEMENTAL INFORMATION

Supplemental information can be found online at https://doi.org/10.1016/j.omtn.2022.10.002.

ACKNOWLEDGMENTS

This work was supported by the Ministry of Science and Technology, Taiwan (108-2314-B-006 -079-MY3, 111-2320-B-006-035-MY3, and 111-2320-B-006-020-MY3). The graphical abstract was created with BioRender.com (https://biorender.com/).

AUTHOR CONTRIBUTIONS

H.-I.Y., P.-Y.H., S.C.C., C.-W.T., and P.-H.C. handled the experiments and analyses. C.-M.C. and S.-H.Y. designed the experiments, oversaw the progress of the study, and drafted the paper. All authors read and approved the final manuscript.

DECLARATION OF INTERESTS

The authors declare no competing interests.

REFERENCES

1. (1993). A novel gene containing a trinucleotide repeat that is expanded and unstable on Huntington's disease chromosomes. The Huntington's disease collaborative research group. Cell *72*, 971–983. https://doi.org/10.1016/0092-8674(93)90585-e.

2. Yang, S.H., and Chan, A.W.S. (2011). Transgenic animal models of Huntington's disease. Curr. Top. Behav. Neurosci. *7*, 61–85. https://doi.org/10.1007/7854_2010_105.

3. Li, S.H., and Li, X.J. (2004). Huntingtin-protein interactions and the pathogenesis of Huntington's disease. Trends Genet. *20*, 146–154. https://doi.org/10.1016/j.tig.2004.01.008.

4. Tung, C.W., Huang, P.Y., Chan, S.C., Cheng, P.H., and Yang, S.H. (2021). The regulatory roles of microRNAs toward pathogenesis and treatments in Huntington's disease. J. Biomed. Sci. *28*, 59. https://doi.org/10.1186/s12929-021-00755-1.

5. Wu, Y.Y., and Kuo, H.C. (2020). Functional roles and networks of non-coding RNAs in the pathogenesis of neurodegenerative diseases. J. Biomed. Sci. *27*, 49. https://doi.org/10.1186/s12929-020-00636-z.

6. Eyileten, C., Sharif, L., Wicik, Z., Jakubik, D., Jarosz-Popek, J., Soplinska, A., Postula, M., Czlonkowska, A., Kaplon-Cieslicka, A., and Mirowska-Guzel, D. (2021). The relation of the brain-derived neurotrophic factor with MicroRNAs in neurodegenerative diseases and ischemic stroke. Mol. Neurobiol. *58*, 329–347. https://doi.org/10.1007/s12035-020-02101-2.

7. Dong, X., and Cong, S. (2018). Bioinformatic analysis of microRNA expression in Huntington's disease. Mol. Med. Rep. *18*, 2857–2865. https://doi.org/10.3892/mmr.2018.9238.

8. Kunkanjanawan, T., Carter, R.L., Prucha, M.S., Yang, J., Parnpai, R., and Chan, A.W.S. (2016). miR-196a ameliorates cytotoxicity and cellular phenotype in transgenic Huntington's disease monkey neural cells. PLoS One *11*, e0162788. https://doi.org/10.1371/journal.pone.0162788.

9. Hoss, A.G., Labadorf, A., Latourelle, J.C., Kartha, V.K., Hadzi, T.C., Gusella, J.F., MacDonald, M.E., Chen, J.F., Akbarian, S., Weng, Z., et al. (2015). miR-10b-5p expression in Huntington's disease brain relates to age of onset and the extent of striatal involvement. BMC Med. Genom. *8*, 10. https://doi.org/10.1186/s12920-015-0083-3.

10. Yusuf, I.O., Chen, H.M., Cheng, P.H., Chang, C.Y., Tsai, S.J., Chuang, J.I., Wu, C.C., Huang, B.M., Sun, H.S., and Yang, S.H. (2019). Fibroblast growth factor 9 activates anti-oxidative functions of Nrf2 through ERK signalling in striatal cell models of Huntington's disease. Free Radic. Biol. Med. *130*, 256–266. https://doi.org/10.1016/j.freeradbiomed.2018.10.455.

11. Miyazaki, Y., Adachi, H., Katsuno, M., Minamiyama, M., Jiang, Y.M., Huang, Z., Doi, H., Matsumoto, S., Kondo, N., Iida, M., et al. (2012). Viral delivery of miR-196a ameliorates the SBMA phenotype via the silencing of CELF2. Nat. Med. *18*, 1136–1141. https://doi.org/10.1038/nm.2791.

12. Fu, M.H., Li, C.L., Lin, H.L., Tsai, S.J., Lai, Y.Y., Chang, Y.F., Cheng, P.H., Chen, C.M., and Yang, S.H. (2015). The potential regulatory mechanisms of miR-196a in Huntington's disease through bioinformatic analyses. PLoS One *10*, e0137637. https://doi.org/10.1371/journal.pone.0137637.

13. Her, L.S., Mao, S.H., Chang, C.Y., Cheng, P.H., Chang, Y.F., Yang, H.I., Chen, C.M., and Yang, S.H. (2017). miR-196a enhances neuronal morphology through suppressing RANBP10 to provide neuroprotection in Huntington's disease. Theranostics *7*, 2452–2462. https://doi.org/10.7150/thno.18813.

14. Cheng, P.H., Li, C.L., Chang, Y.F., Tsai, S.J., Lai, Y.Y., Chan, A.W.S., Chen, C.M., and Yang, S.H. (2013). miR-196a ameliorates phenotypes of Huntington disease in cell, transgenic mouse, and induced pluripotent stem cell models. Am. J. Hum. Genet. *93*, 306–312. https://doi.org/10.1016/j.ajhg.2013.05.025.

15. Blanquie, O., and Bradke, F. (2018). Cytoskeleton dynamics in axon regeneration. Curr. Opin. Neurobiol. *51*, 60–69. https://doi.org/10.1016/j.conb.2018.02.024.

16. Bonini, S.A., Mastinu, A., Ferrari-Toninelli, G., and Memo, M. (2017). Potential role of microtubule stabilizing agents in neurodevelopmental disorders. Int. J. Mol. Sci. *18*, E1627. https://doi.org/10.3390/ijms18081627.

17. Papandréou, M.J., and Leterrier, C. (2018). The functional architecture of axonal actin. Mol. Cell. Neurosci. *91*, 151–159. https://doi.org/10.1016/j.mcn.2018.05.003.

18. Rust, M.B., and Maritzen, T. (2015). Relevance of presynaptic actin dynamics for synapse function and mouse behavior. Exp. Cell Res. *335*, 165–171. https://doi.org/10.1016/j.yexcr.2014.12.020.

19. Fu, M.H., Li, C.L., Lin, H.L., Chen, P.C., Calkins, M.J., Chang, Y.F., Cheng, P.H., and Yang, S.H. (2015). Stem cell transplantation therapy in Parkinson's disease. SpringerPlus *4*, 597. https://doi.org/10.1186/s40064-015-1400-1.

20. Rong, J., McGuire, J.R., Fang, Z.H., Sheng, G., Shin, J.Y., Li, S.H., and Li, X.J. (2006). Regulation of intracellular trafficking of huntingtin-associated protein-1 is critical for TrkA protein levels and neurite outgrowth. J. Neurosci. *26*, 6019–6030. https://doi.org/10.1523/jneurosci.1251-06.2006.

21. DiFiglia, M., Sapp, E., Chase, K.O., Davies, S.W., Bates, G.P., Vonsattel, J.P., and Aronin, N. (1997). Aggregation of huntingtin in neuronal intranuclear inclusions and dystrophic neurites in brain. Science *277*, 1990–1993.

22. Yusuf, I.O., Chen, H.M., Cheng, P.H., Chang, C.Y., Tsai, S.J., Chuang, J.I., Wu, C.C., Huang, B.M., Sun, H.S., Chen, C.M., and Yang, S.H. (2021). FGF9 induces neurite outgrowth upon ERK signaling in knock-in striatal Huntington's disease cells. Life Sci. *267*, 118952. https://doi.org/10.1016/j.lfs.2020.118952.

23. Yusuf, I.O., Chen, H.M., Cheng, P.H., Chang, C.Y., Tsai, S.J., Chuang, J.I., Wu, C.C., Huang, B.M., Sun, H.S., Chen, C.M., and Yang, S.H. (2021). Fibroblast growth factor 9 stimulates neuronal length through NF-kB signaling in striatal cell Huntington's disease models. Mol. Neurobiol. *58*, 2396–2406. https://doi.org/10.1007/s12035-020-02220-w.

24. Farina, K.L., Huttelmaier, S., Musunuru, K., Darnell, R., and Singer, R.H. (2003). Two ZBP1 KH domains facilitate beta-actin mRNA localization, granule formation, and cytoskeletal attachment. J. Cell Biol. *160*, 77–87. https://doi.org/10.1083/jcb.200206003.

25. Chao, J.A., Patskovsky, Y., Patel, V., Levy, M., Almo, S.C., and Singer, R.H. (2010). ZBP1 recognition of beta-actin zipcode induces RNA looping. Genes Dev. *24*, 148–158. https://doi.org/10.1101/gad.1862910.

26. Liao, B., Hu, Y., Herrick, D.J., and Brewer, G. (2005). The RNA-binding protein IMP-3 is a translational activator of insulin-like growth factor II leader-3 mRNA during proliferation of human K562 leukemia cells. J. Biol. Chem. *280*, 18517–18524. https://doi.org/10.1074/jbc.M500270200.

27. Lederer, M., Bley, N., Schleifer, C., and Hüttelmaier, S. (2014). The role of the oncofetal IGF2 mRNA-binding protein 3 (IGF2BP3) in cancer. Semin. Cancer Biol. *29*, 3–12. https://doi.org/10.1016/j.semcancer.2014.07.006.

28. Huang, X., Zhang, H., Guo, X., Zhu, Z., Cai, H., and Kong, X. (2018). Insulin-like growth factor 2 mRNA-binding protein 1 (IGF2BP1) in cancer. J. Hematol. Oncol. *11*, 88. https://doi.org/10.1186/s13045-018-0628-y.

29. Degrauwe, N., Suvà, M.L., Janiszewska, M., Riggi, N., and Stamenkovic, I. (2016). IMPs: an RNA-binding protein family that provides a link between stem cell maintenance in normal development and cancer. Genes Dev. *30*, 2459–2474. https://doi.org/10.1101/gad.287540.116.

30. Schaeffer, D.F., Owen, D.R., Lim, H.J., Buczkowski, A.K., Chung, S.W., Scudamore, C.H., Huntsman, D.G., Ng, S.S.W., and Owen, D.A. (2010). Insulin-like growth factor 2 mRNA binding protein 3 (IGF2BP3) overexpression in pancreatic ductal adenocarcinoma correlates with poor survival. BMC Cancer *10*, 59. https://doi.org/10.1186/1471-2407-10-59.

31. Toledano, H., D'Alterio, C., Czech, B., Levine, E., and Jones, D.L. (2012). The let-7-Imp axis regulates ageing of the Drosophila testis stem-cell niche. Nature *485*, 605–610. https://doi.org/10.1038/nature11061.

32. Boylan, K.L.M., Mische, S.E., Li, M., Marques, G., Morin, X., Chia, W., and Hays, T.S. (2005). A motility screen identifies Drosophila IGF-II mRNA-binding protein, a zip-code-binding protein that functions in oogenesis and synaptogenesis. PLoS Genet. e36. https://doi.org/10.1371/journal.pgen.0040036.eor.

33. Mori, H., Sakakibara, S., Imai, T., Nakamura, Y., Iijima, T., Suzuki, A., Yuasa, Y., Takeda, M., and Okano, H. (2001). Expression of mouse igf2 mRNA-binding protein 3 and its implications for the developing central nervous system. J. Neurosci. Res. *64*, 132–143. https://doi.org/10.1002/jnr.1060.

34. Flores, L.R., Keeling, M.C., Zhang, X., Sliogeryte, K., and Gavara, N. (2019). Lifeact-GFP alters F-actin organization, cellular morphology and biophysical behaviour. Sci. Rep. *9*, 3241. https://doi.org/10.1038/s41598-019-40092-w.

35. Nilufar, S., Morrow, A.A., Lee, J.M., and Perkins, T.J. (2013). FiloDetect: automatic detection of filopodia from fluorescence microscopy images. BMC Syst. Biol. *7*, 66. https://doi.org/10.1186/1752-0509-7-66.

36. Krugmann, S., Jordens, I., Gevaert, K., Driessens, M., Vandekerckhove, J., and Hall, A. (2001). Cdc42 induces filopodia by promoting the formation of an IRSp53:Mena complex. Curr. Biol. *11*, 1645–1655. https://doi.org/10.1016/s0960-9822(01)00506-1.

37. Tang, D.D., and Gunst, S.J. (2004). The small GTPase Cdc42 regulates actin polymerization and tension development during contractile stimulation of smooth muscle. J. Biol. Chem. *279*, 51722–51728. https://doi.org/10.1074/jbc.M408351200.

38. Borovecki, F., Lovrecic, L., Zhou, J., Jeong, H., Then, F., Rosas, H.D., Hersch, S.M., Hogarth, P., Bouzou, B., Jensen, R.V., and Krainc, D. (2005). Genome-wide expression profiling of human blood reveals biomarkers for Huntington's disease. Proc. Natl. Acad. Sci. USA *102*, 11023–11028. https://doi.org/10.1073/pnas.0504921102.

39. Kapitein, L.C., and Hoogenraad, C.C. (2015). Building the neuronal microtubule cytoskeleton. Neuron *87*, 492–506. https://doi.org/10.1016/j.neuron.2015.05.046.

40. Wang, S.E., and Wu, C.H. (2021). Tau phosphorylation and cochlear apoptosis cause hearing loss in 3×Tg-AD Mouse Model of Alzheimer's Disease. Chin. J. Physiol. *64*, 61–71. https://doi.org/10.4103/cjp.Cjp_79_20.

41. Fernandez-Valenzuela, J.J., Sanchez-Varo, R., Muñoz-Castro, C., De Castro, V., Sanchez-Mejias, E., Navarro, V., Jimenez, S., Nuñez-Diaz, C., Gomez-Arboledas, A., Moreno-Gonzalez, I., et al. (2020). Enhancing microtubule stabilization rescues cognitive deficits and ameliorates pathological phenotype in an amyloidogenic Alzheimer's disease model. Sci. Rep. *10*, 14776. https://doi.org/10.1038/s41598-020-71767-4.

42. Reinhardt, L., Kordes, S., Reinhardt, P., Glatza, M., Baumann, M., Drexler, H.C.A., Menninger, S., Zischinsky, G., Eickhoff, J., Fröb, C., et al. (2019). Dual inhibition of GSK3β and CDK5 protects the cytoskeleton of neurons from neuroinflammatory-mediated degeneration in vitro and in vivo. Stem Cell Rep. *12*, 502–517. https://doi.org/10.1016/j.stemcr.2019.01.015.

43. Lin, C.H., Lin, H.I., Chen, M.L., Lai, T.T., Cao, L.P., Farrer, M.J., Wu, R.M., and Chien, C.T. (2016). Lovastatin protects neurite degeneration in LRRK2-G2019S parkinsonism through activating the Akt/Nrf pathway and inhibiting GSK3β activity. Hum. Mol. Genet. *25*, 1965–1978. https://doi.org/10.1093/hmg/ddw068.

44. Dubey, T., and Chinnathambi, S. (2021). Photodynamic sensitizers modulate cytoskeleton structural dynamics in neuronal cells. Cytoskeleton (Hoboken) *78*, 232–248. https://doi.org/10.1002/cm.21655.

45. Ganguly, A., Tang, Y., Wang, L., Ladt, K., Loi, J., Dargent, B., Leterrier, C., and Roy, S. (2015). A dynamic formin-dependent deep F-actin network in axons. J. Cell Biol. *210*, 401–417. https://doi.org/10.1083/jcb.201506110.

46. Fu, Y.T., Zhang, D.Q., Zhou, L., Li, S.J., Sun, H., Liu, X.L., and Zheng, H.B. (2018). Has-MiR-196a-2 is up-regulated and acts as an independent unfavorable prognostic factor in thyroid carcinoma. Eur. Rev. Med. Pharmacol. Sci. *22*, 2707–2714. https://doi.org/10.26355/eurrev_201805_14967.

47. Mueller, D.W., and Bosserhoff, A.K. (2011). MicroRNA miR-196a controls melanoma-associated genes by regulating HOX-C8 expression. Int. J. Cancer *129*, 1064–1074. https://doi.org/10.1002/ijc.25768.

48. Lin, S., Luo, W., Ye, Y., Bekele, E.J., Nie, Q., Li, Y., and Zhang, X. (2017). Let-7b regulates myoblast proliferation by inhibiting IGF2BP3 expression in Dwarf and normal chicken. Front. Physiol. *8*, 477. https://doi.org/10.3389/fphys.2017.00477.

49. Zhang, K., Zhou, M., Chen, H., Wu, G., Chen, K., and Yang, H. (2015). Expression of IMP3 and IGF2 in giant cell tumor of spine is associated with tumor recurrence and angiogenesis. Clin. Transl. Oncol. *17*, 570–575. https://doi.org/10.1007/s12094-015-1280-4.

50. Nielsen, J., Christiansen, J., Lykke-Andersen, J., Johnsen, A.H., Wewer, U.M., and Nielsen, F.C. (1999). A family of insulin-like growth factor II mRNA-binding proteins represses translation in late development. Mol. Cell Biol. *19*, 1262–1270. https://doi.org/10.1128/mcb.19.2.1262.

51. Nielsen, F.C., Nielsen, J., and Christiansen, J. (2001). A family of IGF-II mRNA binding proteins (IMP) involved in RNA trafficking. Scand. J. Clin. Lab. Invest. Suppl. *234*, 93–99.

52. Dütting, S., Gaits-Iacovoni, F., Stegner, D., Popp, M., Antkowiak, A., van Eeuwijk, J.M.M., Nurden, P., Stritt, S., Heib, T., Aurbach, K., et al. (2017). A Cdc42/RhoA

regulatory circuit downstream of glycoprotein Ib guides transendothelial platelet biogenesis. Nat. Commun. *8*, 15838. https://doi.org/10.1038/ncomms15838.

53. Brown, M.D., Cornejo, B.J., Kuhn, T.B., and Bamburg, J.R. (2000). Cdc42 stimulates neurite outgrowth and formation of growth cone filopodia and lamellipodia. J. Neurobiol. *43*, 352–364. https://doi.org/10.1002/1097-4695(20000615)43:4<352::aid-neu4>3.0.co;2-t.

54. Allodi, I., Comley, L., Nichterwitz, S., Nizzardo, M., Simone, C., Benitez, J.A., Cao, M., Corti, S., and Hedlund, E. (2016). Differential neuronal vulnerability identifies IGF-2 as a protective factor in ALS. Sci. Rep. *6*, 25960. https://doi.org/10.1038/srep25960.

55. Mellott, T.J., Pender, S.M., Burke, R.M., Langley, E.A., and Blusztajn, J.K. (2014). IGF2 ameliorates amyloidosis, increases cholinergic marker expression and raises BMP9 and neurotrophin levels in the hippocampus of the APPswePS1dE9 Alzheimer's disease model mice. PLoS One *9*, e94287. https://doi.org/10.1371/journal.pone.0094287.

56. Lu, T.P., Lee, C.Y., Tsai, M.H., Chiu, Y.C., Hsiao, C.K., Lai, L.C., and Chuang, E.Y. (2012). miRSystem: an integrated system for characterizing enriched functions and pathways of microRNA targets. PLoS One *7*, e42390. https://doi.org/10.1371/journal.pone.0042390.

57. Cheng, P.H., Chang, Y.F., Mao, S.H., Lin, H.L., Chen, C.M., and Yang, S.H. (2016). Lentiviral transgenesis in mice via a simple method of viral concentration. Theriogenology *86*, 1427–1435. https://doi.org/10.1016/j.theriogenology.2016.04.088.

58. Mangiarini, L., Sathasivam, K., Seller, M., Cozens, B., Harper, A., Hetherington, C., Lawton, M., Trottier, Y., Lehrach, H., Davies, S.W., and Bates, G.P. (1996). Exon 1 of the HD gene with an expanded CAG repeat is sufficient to cause a progressive neurological phenotype in transgenic mice. Cell *87*, 493–506. https://doi.org/10.1016/s0092-8674(00)81369-0.